Proceedings of the 2007 IEEE Symposium on Computational Intelligence in Image and Signal Processing (CIISP 2007)

A Pilot Study of Automatic Lung Tumor Segmentation from Positron Emission Tomography Images using Standard Uptake Values

Aparna Kanakatte[†§], Jayavardhana Gubbi[‡], Nallasamy Mani[†], Tomas Kron[⋆], David Binns[⋆]
[†]Dept of Electrical and Computer Systems, Monash University, Clayton, Victoria - 3800, Australia.
[‡]Dept of Electrical and Electronics Engineering, The University of Melbourne, Parville, Victoria - 3010, Australia.
[⋆]Peter MacCallum Cancer Centre, St Andrews Place, East Melbourne, Victoria - 3002, Australia.
[§]Aparna.Gurumurthy@eng.monash.edu.au

Abstract— **Positron Emission Tomography (PET) is a medical imaging procedure that shows the physiological function of an organ or tissue. The role of PET during the past decade has evolved rapidly in the detection of lung tumors but the research on quantitative evaluation of PET images is still in its infancy. PET commonly involves scanning the patient after administration of a radioactive analogue of glucose called fluoro deoxy-glucose (FDG). Tumor cells metabolise more glucose than most normal cells. In PET lung images the heart is often visible and because of its constant pumping of blood it requires more glucose and hence both the tumor and the heart appear brighter than the rest in the PET image. In this paper we present a novel segmentation scheme for detecting the tumor alone in lung PET images using standard uptake values (SUV) and connected component analysis. We perform the segmentation in two steps. In coarse segmentation, a non linear scaling of SUV values is performed and then a threshold is chosen adaptively to convert the gray image into the binary image. Fine segmentation is performed on the coarse segmented data in order to narrow down the region of interest using connected component labeling. To our knowledge no one has used connected component analysis for segmenting PET images. We compare our proposed scheme with several commonly used medical image segmentation techniques like threshold, sobel edge detector, laplacian of gaussian (LoG) edge detector, region growing and SUV based segmentation (applied only to PET as SUV is specific to PET). One of the problems in lung tumor detection is the presence of the heart in the image which accumulates activity and often gets recognized as a hot spot (a probable tumor). All the other segmentation schemes detected both the heart and the tumor as hot spots while our segmentation scheme detected the tumor alone as the hot spot. The preliminary study of the proposed scheme has yielded very promising results and will be studied for more lung tumor detection scenarios in future.**

I. Introduction

Lung cancer is caused by the rapid growth and division of cells that make up the lungs. It is one of the most lethal of cancers worldwide. According to this year's survey from the American Cancer Society, about 3 million persons have lung cancer and the majority of them are residing in the developed countries. Findings from the U.S. National Cancer Institute (NCI) indicate the upward trend in cancer-related death is due to the rapidly increasing rate of lung cancer mortality. Only one in ten patients diagnosed with this disease will survive the next □ve years. Although research showed that previously this affected predominately men, the lung cancer rate for women has been increasing in the last few decades due to the rise in female smokers. From the recent survey conducted by *National Lung Cancer Research*, more woman die of lung cancer than any other cancer, including breast, ovarian and uterine cancers combined. Current research indicates that the greatest impact on this cancer is long-term exposure to inhaled carcinogens, the most common being tobacco smoke. Treatment and prognosis depend upon the histological type of cancer and the stage or degree of spread. Surgery, chemotherapy and/or radiotherapy are the possible treatments for this deadly disease.

Medical imaging modalities like Computed Tomography (CT), Magnetic Resonance Imaging (MRI) and PET are an integral part of cancer diagnosis and treatment planning providing an effective assessment for cancer treatment. Lardinois *et.al.* [8] have shown that FDG-PET (Fluoro deoxy glucose) is very accurate in classifying lung nodules by differentiating between benign and malignant tumors. PET is a medical imaging procedure that shows the biological function of an organ or tissue rather than its anatomical structure as shown by CT. The poor anatomical information obtained in the PET scanner is complemented by X-ray CT imaging. Then the two images were manually registered to locate the tumor and its relative location to the anatomy. The success of this registration depended on both the scanners having the same patient position. However, a combined PET/CT system has both CT and PET scanners integrated together and this generates perfectly co-registered images taken during contemporaneous scanning, provided that the patient does not move. Hence integrated CT/PET scanners are rapidly becoming popular in hospitals. Steinert [19] has stated that combined PET/CT is the best diagnostic instrument to detect lung cancer. PET has improved early diagnosis and follow up of lung cancer. PET scanning with FDG has other validated clinical applications in other cancers along with uses in neurology and cardiology. Researchers are exploring the option of extending PET with the use of other radiopharmaceuticals that target other features of cancer physiology. PET also has a signi□cant role in monitoring the effectiveness of therapy. Reduction in FDG uptake following treatment has a good correlation with

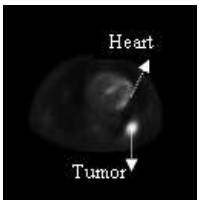

Fig. 1. Labeled PET image

effective therapy and improved outcomes.

Segmentation is a preliminary stage for visualization or quanti□cation of medical images for computer-aided diagnosis and therapy planning. Image segmentation plays a crucial role in automatically delineating the anatomical structures or regions of interest. Pal *et. al.* [11] in their review paper have evaluated various segmentation techniques. Pham *et.al.* [13] have presented various techniques used in medical image segmentation. They divide segmentation methods into eight categories namely thresholding approaches, region growing approaches, classi□ers, clustering approaches, Markov random □eld (MRF) models, arti□cial neural networks, deformable models and atlas guided approaches. Most of these techniques are applied to MRI [13] [12], Ultrasound or CT and not on PET images since PET only became widely available recently.

FDG-PET shows the biological function or metabolism of an organ. In general tumor cells metabolise more glucose than normal or healthy cells [18]. In lung PET images, the heart is often visible and because of constant pumping of blood it metabolises more glucose. Hence both the tumor and heart appear brighter than the rest of the cells as shown in □gure 1. As a result of this both the heart and tumor are detected as hot spots (probable tumors) in the segmentation schemes. This complicates the segmentation of lung lesions. Guan *et.al.* [4] have proposed an automatic hot spot detection and segmentation of whole body PET images using threshold and the Hidden Markov model (HMM). They compare the □xed PET pixel data threshold and the □xed standard uptake values (SUV) threshold for segmenting hot spots. In this paper we intend to segment the tumor from lung PET images. We propose a novel segmentation technique and compare some of the standard segmentation schemes applied on various medical images with our scheme. We have shown some segmented images from our scheme and various compared schemes. Our segmentation scheme was able to delineate the exact tumor area which no other compared schemes were able to achieve. This paper is organised as follows: Section 2 describes the detailed calculation of SUV and image acquisition is explained in section 3. Several standard segmentation schemes like gray intensity thresholding, SUV based segmentation, edge detectors, region growing method are discussed in section 4. The proposed two stage segmentation scheme is described in section 5. Evaluation of the proposed scheme is discussed in section 6 and conclusions are given in section 7.

II. Calculation of Standard Uptake Value (SUV)

Standard Uptake Values [5] are frequently used for FDG PET to evaluate uptake quantitatively. Tumor cells metabolise more glucose than normal or healthy cells [18]. Hence, in general, if the tumor is present it appears brighter than healthy cells in a PET image. This high uptake is commonly used to differentiate healthy tissue from a tumor. SUV is also known as the differential uptake ratio, the differential absorption ratio, the dose uptake ratio or the dose absorption ratio.

Each pixel in the PET image is represented by 15 bits and has intensity values in the range from 0 to 32767. In order to obtain the tissue activity in each point, Bq/cc, units as measured by the PET/CT scanner, the pixel data is rescaled by the tags 'Rescale Slope' and 'Rescale Intercept' available from the dicom header [1]. These tags varies for every image slice. Tissue activity is calculated using formula 1.

$$Y = ax + b \tag{1}$$

where x is the original pixel intensity value, Y is the tissue activity concentration in Bq/cc, a is the rescale slope and b is the rescale intercept for each image slice of the PET scan.

The value of SUV is a quantitative way of comparing tumors across different patients [6]. Using patient body weight is most common in calculating SUV, though some physicians prefer to use body surface, or lean body mass instead. For each voxel, SUV is calculated assuming $1cc = 1g$ and applying equation 2.

$$SUV = \frac{YW}{D} \tag{2}$$

where Y is the activity concentration in Bq/cc calculated from equation 1, W is the patient weight in kg and D is the injected dose at scan start (Bq). With this de□nition, if the injected dose is equally distributed over the whole body, then each point will have an SUV of 1. The injected dose is the activity in the dose at the time of injection. The time between injection and scan start varies between one to two hours depending on the patient and during this time the tracer substance is distributed over the whole body. The activity of the injected dose at scan start is given by equations 3 and 4

$$D = d_{inj}.e^{-\lambda.t_{diff}} \tag{3}$$

$$\lambda = \frac{\log 2}{T_{1/2}} \tag{4}$$

where d_{inj} is the activity of the injected dose at the injection time, t_{diff} is the time between the injection and the scan start time and $T_{1/2}$ is the half life for F-18 (FDG). When describing the tumor, physicians often take the maximum SUV in the area of the hot spot which usually does not exceed 15. In general the higher the SUV, the more aggressive is the tumor. So an SUV of 15 is considered to be a very aggressive tumor while SUV between 7 and 8 is typical.

The SUV value is also used to distinguish between the malignant and benign tumor. An SUV value of 2.5 [10] is often considered as the threshold (cutoff) to distinguish between benign and malignancy. SUV runs into controversy [7] in

de□ning this threshold value because of the various physical parameters like patient weight, glucose level, length of the uptake period and body composition that are involved for this value calculation. The threshold value varies for different body organs. If the liver is taken into consideration the threshold will be different as normal tissue will have an SUV value greater than 2.5.

III. Image Acquisition

PET imaging was conducted on a Discovery STE8 PET/CT scanner manufactured by GE Medical systems. Commonly, the patient is scanned after about 1 to 1.5 hours of administering $320MBq$ of deoxy-2-[18F]□uoro-D-glucose (FDG) to the patient. The patient was instructed by the physician to fast a maximum of four hours before scanning. Five to six frames of whole-body 2D (with septa) emission data was obtained. The scanner takes about 5 minutes for the acquisition of each frame. The total scanning time is approximately around 40 minutes per patient. The images are captured in the form of many slices (2D mode) with the thickness of each slice being $3.27mm$. All the images obtained were corrected for attenuation. Only lung images slices were then segregated from the whole body image and were used for testing the segmentation schemes. PET images obtained for this study are from the Peter MacCallum Cancer Centre in Melbourne. The patient identi□ers were removed from the images prior to analysis.

IV. Segmentation Techniques

Segmentation is the process of partitioning the image into some non intersecting regions. Each segmented region is homogeneous with respect to a given characteristic such as intensity, gray tone or texture. The union of no two adjacent regions is homogeneous. Fu [3] has stated that most image segmentation approaches can be placed in one of three categories namely 'Thresholding or Clustering', 'Edge detection' and 'Region-based segmentation'. In this paper we introduce a novel segmentation technique and compare this with a number of commonly used segmentation methods applied only on the lung PET images. The techniques are gray intensity threshold and SUV based segmentation (category: Thresholding), sobel edge detector and laplacian of gaussian (LoG) edge detector (category: Edge detection), basic region growing (category: Region based segmentation)

A. Gray Intensity Adaptive Threshold

Thresholding is one of the simplest and most commonly used techniques for image segmentation. In this method, the image is divided into a foreground region (or region of interest) and background region based on the intensity threshold value. The resultant image is a binary image. A threshold value can be chosen either manually by a trial and error process or automatically by analysis of the histogram, mean and median of the image.

The pixel data obtained from PET is represented in 15 bits and has intensity values between 0 - 32767. For ease of display and viewing this is converted to a gray scale image with intensity values between 0 - 255 . Guan *et.al.* [4] uses the original 15 bit data image and applies a □xed pixel data threshold value of 3000 to convert the gray image into a binary image. Selecting a □xed threshold may not be an optimal approach. We intend to automatically select the threshold adaptively based on the histogram of the image. This is done by analyzing the gray intensity histogram of the image and □tting two Gaussian curves to the histogram as shown in □gure 2. The □rst Gaussian (Gaussian curve 1) is □tted for gray values $0-200$ and the second (Gaussian curve 2) between the values $100-255$. The threshold value T (T in □gure 2), is the average of the two Gaussian means. This is used to binarize the image. In □gure 2 the x axis is the gray values and the y axis is the values of the scaled histogram. The scaling is done in order to show the □tting of the two gaussian curves clearly. The binarisation is given by equation 5.

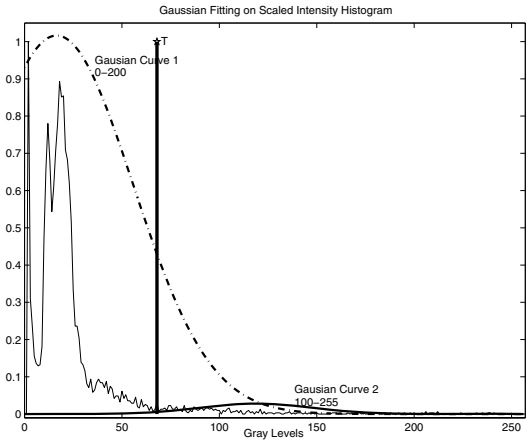

Fig. 2. Gaussian □tting on scaled histogram

$$Binary[i][j] = \begin{cases} 1, & \text{if Image}[i][j] \geq T(Foreground) \\ 0, & \text{if Image}[i][j] < T(Background) \end{cases} \quad (5)$$

where i is the row and j is the column of the pixel under consideration.

B. SUV-based Segmentation

As stated earlier SUV is a representation of the uptake in a given region of interest related to the average uptake throughout the body. Tumor cells absorb more glucose than normal cells and hence will have higher SUV value. Guan *et.al.* [4] uses an SUV threshold of 2.5 on the whole body FDG-PET image for segmentation. However, this threshold of 2.5 applied to the whole body image might falter when the liver is taken into consideration as normal cell will have SUV higher than 2.5. As our intention is to detect the presence of a tumor in the lung region alone a threshold of SUV greater than or equal to 2.5 is selected to differentiate between healthy and suspected tumor cells. This threshold value is chosen based on the experience at PeterMac Cancer Centre and is valid only on lung images.

The calculation of SUV is explained in detail in section 3. If the SUV value is greater than or equal to 2.5, the pixel is taken as the foreground; otherwise, it is taken as background. Binarisation of the original image is accomplished using the equation 6.

$$Binary[i][j] = \begin{cases} 1, & \text{if suvImage}[i][j] \geq 2.5 \\ 0, & \text{if suvImage}[i][j] < 2.5 \end{cases} \quad (6)$$

where i is the row and j is the column of the pixel under consideration.

C. Edge Detection

An edge can be de□ned as a change in intensity taking place over a number of pixels. We have implemented Sobel and Laplacian of Gaussian edge detectors for comparative study. Sobel edge detection [16] is based upon the □rst derivative of the intensity, *i.e* it gives the intensity gradient of the original data. The Sobel operator approximates the gradient by using each row and a column mask for the horizontal and the vertical directions.

Laplacian of Gaussian (LoG) [20] is an advanced second derivative edge detector because they are algorithmic in nature, which basically means they require multiple steps. LoG is essentially the rate of change in the intensity gradient. This is performed in two steps

- The image is convolved with a Gaussian smoothing □lter
- The image is convolved with a Laplacian mask

By pre-processing with a Gaussian □lter the noise effects are mitigated and the Lapacian mask is then used to enhance the edges.

These two edge detectors can be easily implemented by using masks which are available in any standard image processing books [16] [20]. Both Sobel and LoG edge detectors are applied to the gray intensity image. There is a lot of noise in the LoG output image compared to Sobel (shown in □gures 4 and 5) because of the sensitivity of the second derivative. Both techniques failed to detect the required region of interest and the output images require post processing.

D. Region Growing

Region Growing [15], [13] is one of the most commonly used segmentation scheme for medical images. This is a technique for extracting a region of interest based on associated region characteristics, such as homogeneity of gray scale, color, texture, shape *etc*. This technique is better suitable for noisy images where edges are not clearly visible. The most basic form of region growing is solely based on thresholding and the connectivity criteria. Connectivity de□nes regions by recursively considering pixels that are connected to the seed pixel [17]. A pixel is connected to this seed pixel if it satis□es the thresholding condition and the connectivity criteria (either 4 or 8 connectivity). Till recently, the seed point was manually selected by the operator but now there are many algorithms to automatically detect the seed point. The ef□ciency of segmentation is higher for manually detected seed point than the ones detected automatically. Even today some software used in Medical hospitals detect seed point manually for region growing segmentation.

A basic region growing algorithm using gray level thresholding and connectivity has been employed for comparative study. Various gray intensity threshold values between 10 and 100 and connectivity of 4 and 8 have been tested. By trial and error process we have chosen a homogeneity criteria (threshold) of 50 and connectivity criteria of 4 as it performed well on various sets of images. This is a computationally intense technique. If the homogeneity criteria is not chosen properly then the region can get either over segmented (detecting false tumor area) or under segmented (not detecting the tumor area). The results obtained from this scheme is not consistent *i.e.* for certain images it successfully detects the tumor alone, but on most of the images it detects both the tumor and heart. In some cases the tumor gets over segmented and in certain cases gets under segmented. Obtaining a suitable homogeneity criteria is a very challenging task.

As the results from the standard techniques failed to detect the exact tumor area alone, we propose a new scheme that can detect the tumor in the lung PET images.

V. Proposed Segmentation Scheme

We introduce a novel segmentation scheme which is carried out in two stages namely coarse and □ne segmentation. In coarse segmentation, we enhance the image and then convert it to a binary image using an adaptively chosen threshold. In □ne segmentation, this binary image undergoes connected component labeling for segmenting the region of interest.

1) Coarse Segmentation: In coarse segmentation we convert the original 15 bit image into a binary image with the region of interest or tumor being the foreground and the rest as back ground. This binarization is done in two steps

- The original image is enhanced and converted to gray scale
- The gray scale image is converted to binary image using an adaptively chosen threshold

We apply an enhancement technique which emphasizes the foreground and reduces the background of the original image. This is done by multiplying the SUV values by the original pixel values. The resultant image will have a reduced background and a dominant foreground as shown in □gure 3. It can be noted that SUV values are derived from the 15 bit intensity data obtained from the PET image. Hence, this enhancement is due to the non linear scaling of SUV values. This enhanced 15 bit image is converted to a 8 bit gray scale image for display purposes.

The next step is to convert this gray scale into a binary image. This is done by adaptively choosing the intensity threshold according to the image by □tting two gaussian curves as explained in Section 4*A*. The average of the mean of these two curves gives the intensity threshold (T). This threshold is used to convert the enhanced image into a binary image using equation 5. By the end of this scheme, we clearly have the tumor being recognised as hot spot. In some cases small parts

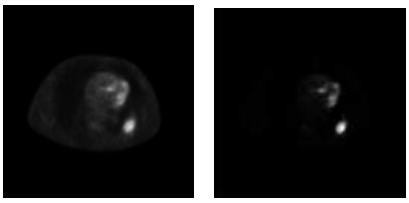

(a) Original Image (b) Enhanced Image

Fig. 3. Proposed enhancement output

of heart get segmented. In order to eliminate this and detect the tumor alone we require fine segmentation.

2) Fine Segmentation: Fine segmentation involves labeling the binary image obtained from coarse segmentation using connected component labeling. To our knowledge this has not been used in PET image segmentation. The motivation for using this is to narrow down the region of interest and eliminate noise if it is present after coarse segmentation. The connected component labeling algorithm is explained in detail here.

Connected components [9] [2] [14] are defined as regions with uniform pixel values grouped into components based on either 8 or 4 connectivity. Connected component analysis [2] is a method of labeling which works on both binary and gray scale images. All the pixels in a connected component share similar pixel or intensity values V and are in some way connected with each other. For a binary image this value $V = 1$

We have applied this technique on a binary image and grouped the pixels into components based on 8 - connectivity. The 8 neighbors of a pixel 'p' with co-ordinates (x, y) denoted by $N_8(p)$ is defined as:

$$N_8(p) = N_8(x, y) = I(x + \alpha, y + \beta) \begin{cases} -1 \leq \alpha \leq 1 \\ -1 \leq \beta \leq 1 \end{cases} \quad (7)$$

Two pixels p and q are 8-connected if $q \in N_8(p) \Rightarrow p \in N_8(q)$ and both have the same values of either 1 or 0. A path from pixel p with co-ordinates (x_0, y_0) to pixel q with co-ordinates (x_n, y_n) exists if there exists a sequence of distinct pixels $(x_0, y_0), (x_1, y_1), (x_2, y_2), ..., (x_{n-1}, y_{n-1}), (x_n, y_n)$ such that (x_i, y_i) is 8-connected to (x_{i-1}, y_{i-1}) for all i satisfying $1 \leq i \leq n$.

The labeling starts by vertically scanning each column of the image. The scanning is done from left to right. Lets assume that the first ON (i.e $V = 1$) pixel is found at point z. The eight neighbors of z are examined and the labeling occurs as follows:

- If all eight neighbors are 0, a new label is assigned to z,
- If only one neighbor has $V = 1$, its label is assigned to z,
- If two or more of the neighbors have $V = 1$, one of the labels is assigned to z and a note of the equivalences is made.

After scanning the whole image, the equivalent label pairs are sorted into equivalence classes and a unique label is assigned to each class. As a final step, a second scan is made through the image, during which each label is replaced by the label assigned to its equivalence classes. For the pseudocode of the method, the reader is referred to [14].

After completing the labeling on the coarse segmented data, the area of each connected cluster is calculated. If this area is less than 10 pixels then the segmented cluster is treated as noise. By testing on various images we have chosen this area of 10 pixels. Using this technique, a lot of fine noise present during coarse segmentation is reduced substantially. The importance of this can be seen in the output of the two edge detection operators used, where lots of noise has been detected. This two level segmentation technique segments the tumor alone for most of the images tested, while all the other compared segmentation schemes failed to detect this.

VI. Evaluation of the proposed scheme

The results of the above compared schemes are applied on 44 image slices containing the tumor and heart. For clarity, results from two slices are shown in figures 4 and 5. Figure (a) is the original PET image obtained from the scanner. Figure (b) is the output of gray intensity threshold and figure (c) is the output from the SUV threshold image. Figures (d) and (e) are from the Sobel and the Laplacian of Gaussian (LoG) edge detectors respectively. Figure (f) is the output from the region growing technique. The last two figures (g) and (h) are from the proposed two level coarse and fine segmentation scheme. It can be clearly seen that certain parts of the heart region appears brighter than the rest in the original image. Both the edge detection operators failed to detect a clear region of interest. The gray intensity and SUV threshold detected both heart region and tumor as the hot spot for both the slices. Region growing technique detected the tumor alone in both slices. However, it can be clearly seen that the tumor is under-segmented in figure 5 and over-segmented in figure 4. Our segmentation scheme detected tumor alone in both the slices.

VII. Conclusions

In this paper, we have proposed a new two stage segmentation scheme for lung tumor detection. We have introduced an enhancement scheme to enhance the foreground and reduce the background in the PET images using the SUV values. We have also introduced connected component labeling to narrow down the region of interest and eliminate some noise if present during coarse segmentation which to our knowledge has not been used on PET image segmentation. The proposed scheme was compared with various standard schemes like thresholding, SUV based segmentation, region growing and edge detectors used in medical image segmentation. Preliminary evaluation of this scheme resulted in separation of the tumor and the heart allowing the segmentation of the tumor alone indicating that this technique is very promising. The critical parameter 'cutoff threshold' is chosen adaptively according to different images making this a robust and reliable technique which can easily be adapted to different PET imaging systems.

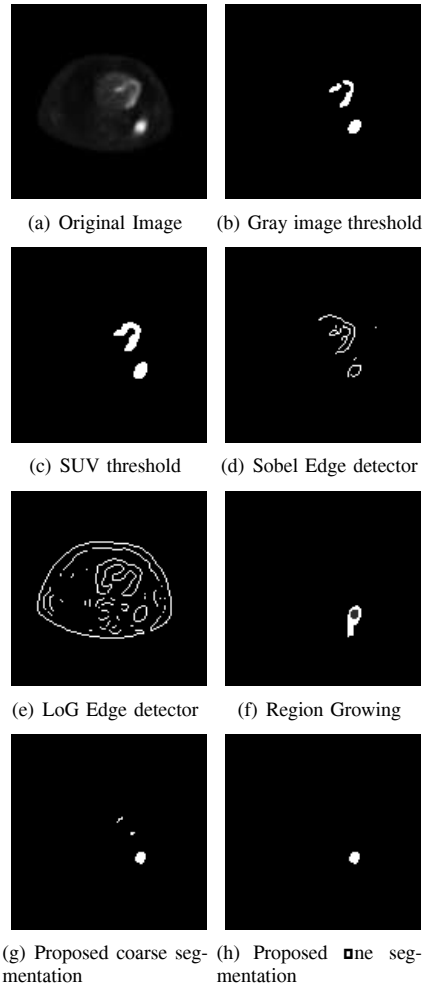

(a) Original Image (b) Gray image threshold

(c) SUV threshold (d) Sobel Edge detector

(e) LoG Edge detector (f) Region Growing

(g) Proposed coarse segmentation (h) Proposed fine segmentation

Fig. 4. Outputs of various compared and our proposed scheme on Slice 15

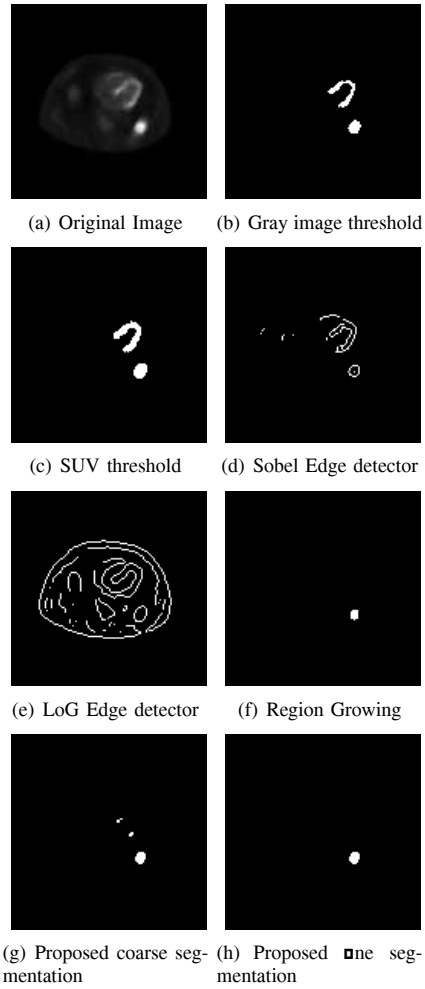

(a) Original Image (b) Gray image threshold

(c) SUV threshold (d) Sobel Edge detector

(e) LoG Edge detector (f) Region Growing

(g) Proposed coarse segmentation (h) Proposed fine segmentation

Fig. 5. Outputs of various compared and our proposed scheme on Slice 18

REFERENCES

[1] D. A. Clunie. *Dicom Structured Reporting*. Pennsylvania: PixelMed, 2000.

[2] R. Fisher, S. Perkins, A. Walker, and E. Wolfart. Informatics homepage server *(http://homepages.inf.ed.ac.uk/rbf/HIPR2/label.htm)*, 2003.

[3] K. S. Fu and J. K. Mui. A survey on image segmentation. *Pattern Recognition*, 13:3–16, 1981.

[4] H. Guan, T. Kubota, X. Huang, X. S. Zhou, and M. Turk. Automatic hot spot detection and segmentation in whole body fdg-pet images. In *Proceedings of the IEEE International Conference on Image Processing (ICIP)*, 2006.

[5] S-C. Huang. Anatomy of suv. *Nuclear Medicine and Biology*, 27:643–646, 2000.

[6] D. Jakobsson and F. Olofsson. Decision support system for lung cancer using pet/ct images. In *Masters Thesis, Lund University of Technology*. 2004.

[7] J. W. Keyes Jr. *SUV*: Standard uptake or silly useless value. *Nuclear Medicine*, 36(10):1836–1839, 1995.

[8] D. Lardinois, W. Weder, and T. F. Hany. Staging of non small cell lung cancer with integrated positron emission tomography and computed tomography. *The New England Journal of Medicine*, 348:2500–2507, 2003.

[9] K. Mahata. Tamil optical character recognition system on printed text. In *Master of Engineering Thesis, Indian Institute of Science*. 2000.

[10] A. Matthies, M. Hickeson, A. Cuchiara, and A. Alavi. Dual time point 18f-fdg pet for evaluation of pulmonary nodules. *Nuclear Medicine*, 43(7):871–875, 2002.

[11] N. R. Pal and S. K. Pal. A review of image segmentation techniques. *Pattern Recognition*, 26(9):1277–1294, 1993.

[12] X. M. Pardo, D. Cabello, and J. Heras. An integration scheme for biomedical computed tomography image segmentation. *Computing and Information Technology (CIT)*, 7(4):295–309, 1999.

[13] D. L. Pham, C. Xu, and J. L. Prince. Current methods in medical image segmentation. *Annual Review of Biomedical Engineering*, 2:315–337, 2000.

[14] I. Pitas. *Digital Image Processing Algorithms and Applications*. A Wiley Interscience publication, 2000.

[15] R. Pohle and K. D. Toennies. Segmentation of medical images using adaptive region growing. In *Proceedings of SPIE(Medical Imaging)*, 2001.

[16] W. K. Pratt. *Digital Image Processing*. Wiley Interscience, 2001.

[17] R. A. Robb. *Biomedical Imaging, Visualisation and Analysis*. Wiley-Liss, 2000.

[18] R. B. Shalom, A. Y. Valdivia, and M. D. Blaufox. Pet imaging in oncology. *Seminars in Nuclear Medicine*, 30(3):150–185, 2000.

[19] H. C. Steinert. Pet in lung cancer. *Chang Gung Medical Journal*, 28(5):296–305, 2005.

[20] S. E. Umbaugh. *Computer imaging: Digital Image Analysis and Processing*. Boca Raton: Taylor and Francis, 2005.